

# Neutralino/chargino pair production at NLO+NLL with resummation-improved PDFs for LHC Run II

J. Fiaschi<sup>1,\*</sup> and M. Klasen<sup>1,†</sup>

<sup>1</sup>*Institut für Theoretische Physik, Westfälische Wilhelms-Universität Münster,  
Wilhelm-Klemm-Straße 9, D-48149 Münster, Germany*

(Dated: August 16, 2018)

## Abstract

We make use of recently released parton density functions (PDFs) with threshold-resummation improvement to consistently calculate theoretical predictions for neutralino and chargino pair production at next-to-leading order and next-to-leading logarithmic accuracy. The updated cross sections have been computed for experimentally relevant higgsino and gaugino search channels at the ongoing Run II of the LHC. A factorisation method is applied to exploit the smaller PDF uncertainty of the global PDF sets and to avoid complications arising in the refitting of threshold-resummation improved PDF replicas in Mellin space. The reduction of the scale uncertainty due to the resummation is, however, explicitly taken into account. As expected, the resummation contributions in the PDF fits partially compensate the cross section enhancements induced by those in the partonic matrix elements.

arXiv:1805.11322v2 [hep-ph] 15 Aug 2018

---

\* fiaschi@uni-muenster.de

† michael.klasen@uni-muenster.de

## I. INTRODUCTION

The Minimal Supersymmetric Standard Model (MSSM) is a theoretically and phenomenologically well motivated extension of the Standard Model (SM) of particle physics [1, 2]. It predicts in particular fermionic partners of the neutral and charged gauge and Higgs bosons called gauginos and higgsinos, whose lightest neutral mass eigenstate, the lightest neutralino, is one of the best studied dark matter candidates [3–6]. Heavier neutralinos and charginos decay typically into multilepton final states and missing transverse momentum. Searches for gaugino- [7, 8] or higgsino-like particles [9, 10] are important physics goals at the LHC. They are often carried out in the framework of simplified models [11, 12]. Care must, however, be taken that the theoretical assumptions are not overly simplified [13].

Experimental measurements of supersymmetric (SUSY) production cross sections at the ongoing Run II of the LHC require precise theoretical calculations at the level of next-to-leading order (NLO) QCD and beyond [14–23]. In the perturbative expansion, logarithmically enhanced terms appear beyond leading order in the strong coupling constant  $\alpha_s$ , whose contributions can be sizeable close to production threshold or at small transverse momentum of the produced SUSY particle pair. Their effect on neutralino, chargino [24–29], slepton [30–37], squark, gluino [38–41], stop [42, 43] and also new gauge boson production [44–47] has been taken into account to all orders with resummation techniques to next-to-leading logarithmic (NLL) accuracy and beyond, and the results for the electroweak production channels have been made publicly available with the code RESUMMINO [48]. Parton showers also partially resum logarithmically enhanced contributions, and complementary NLO calculations with parton showers have been performed for squark [49, 50], slepton [51] and gaugino pair production [52, 53]. The effect of higher order QCD corrections is generally to enhance the theoretical estimations for the cross sections, while on the other hand they reduce the dependence of the results on the choice of the unphysical renormalisation and factorisation scales.

A consistent prediction of hadronic cross sections would in principle require the same precision in the calculation of the partonic matrix elements of the specific process as in the determination of the parton density functions (PDFs). For this purpose some examples of threshold-resummation improved PDFs have been recently released. In this work we will make use of the NNPDF30\_nlo\_disdytop and NNPDF30\_nll\_disdytop PDF sets [36], which have been obtained by the NNPDF collaboration with partonic matrix elements computed respectively at NLO and NLO+NLL in the fits of experimental data. Unfortunately, NLO+NLL accuracy is only readily available for a rather small subset of relevant processes. Therefore, only part of the available experimental data can enter in a consistent NLO+NLL fit. In particular, the resummed PDF fits rely only on data from deep-inelastic scattering (DIS), the Drell-Yan (DY) process and top-quark pair production. Consequently, the reduction of the input data set leads to a larger PDF error in comparison with a global PDF set.

In this work, we present updated and consistent results for the cross sections of neutralino and chargino production at NLO+NLL for Run II of the LHC. We adopt the  $K$ -factor method already discussed in the literature [54], which will allow for a straightforward rescaling of the fixed-order calculations to consistent NLO+NLL results. The neutralinos and charginos are in general a linear superposition of SM superpartners. Following recent experimental analyses, we consider here two specific scenarios where they are dominated by either the higgsino or the gaugino content. Moreover, we will work with the simplified

models used in the experimental analyses of the ATLAS and CMS collaborations, where the produced neutralinos and charginos are similar in mass, while most other SUSY particles are decoupled. While the gauginos are assumed to decay to the lightest SUSY particle (LSP) through intermediate (s)taus [7], the higgsinos are assumed to decay to a not much lighter LSP producing soft leptons [10]. The associated experimental analyses lead to quite different constraints on the SUSY particle masses.

This paper is organised as follows: In Sec. II, we review the  $K$ -factor method to merge the effect of a consistent resummation both in the PDFs and in the partonic matrix elements with the smaller PDF error of the global set and with a reliable estimate of the scale uncertainty. In Sec. III, we present our numerical results for differential and total cross sections for higgsino pair production at Run II of the LHC, i.e.  $pp$  collisions with 13 TeV centre-of-mass energy, for a range of particles masses that is relevant for current and future experimental searches. Similarly in Sec. IV, we present the results for a typical process in the scenario where the neutralinos and charginos have a large gaugino content. Our conclusions are given in Sec. V.

## II. THEORETICAL METHOD

The aim of this work is to study the impact of threshold-resummation improved PDFs in the calculation of SUSY processes involving neutralinos and charginos as well as updating NLO+NLL predictions for these cross sections for ongoing searches at Run II of the LHC, i.e. for proton-proton collisions with a centre-of-mass energy of 13 TeV. For this purpose we adopt as our PDF baseline the recent global NNPDF3.0 PDF set, which includes data from ATLAS and CMS analyses on jet, vector-boson and top-quark production [55]. We study the changes that arise when we employ the threshold-resummation improved PDF set NNPDF30\_nll\_disdytop together with its fixed-order version NNPDF30\_nlo\_disdytop [36]. The resummed PDF sets are obtained from a reduced data set involving deep-inelastic scattering (DIS), Drell-Yan (DY) and top-quark pair production data, as these are the sole processes for which an analytic expression of the matrix element at NLO+NLL is available. The reduction of the data sets adopted in the fit of the threshold-resummation improved PDF sets leads to a larger PDF error with respect to the global set.

In order to combine the smaller PDF error of the global PDF sets with the effect of the resummation in the fit of the new PDF sets, we follow the approach described in Ref. [54], where the authors introduce a factorisation ( $K$ -factor) method. We define the same  $K$ -factor in Eq. (2.1),

$$K = \frac{\sigma(\text{NLO} + \text{NLL})_{\text{NLO global}}}{\sigma(\text{NLO})_{\text{NLO global}}} \cdot \frac{\sigma(\text{NLO} + \text{NLL})_{\text{NLO+NLL reduced}}}{\sigma(\text{NLO} + \text{NLL})_{\text{NLO reduced}}}, \quad (2.1)$$

which can be used to obtain an approximate result for a consistent NLO+NLL cross section via

$$\sigma(\text{NLO} + \text{NLL})_{\text{NLL+NLO global}} = K \cdot \sigma(\text{NLO})_{\text{NLO global}}. \quad (2.2)$$

This method also allows to rescale the PDF uncertainty extracted from the global set to a consistent NLO+NLL result. The benefits are twofold: On the one hand, the relative size of the PDF uncertainties is obtained only from the global set, which is affected by a smaller PDF error. On the other hand, we avoid refitting the NNPDF replicas in Mellin space, which typically leads to some convergence issues [35].

The other main source of theoretical uncertainty is the freedom in the choice of the unphysical factorisation and renormalisation scales. This uncertainty will not be rescaled from the NLO results through the  $K$ -factor. Instead it will be computed directly. The resummation procedure typically reduces the dependence of the results on the choice of the scales. Thus we will explicitly estimate the scale uncertainties on the NLO+NLL result, following the seven-point method, i.e. varying the two scales by relative factors of two, but not four about the central scale, taken to be the average mass of the two produced SUSY particles. The total theoretical error will be taken as the sum in quadrature of the PDF and scale uncertainties.

### III. HIGGSINO PAIR PRODUCTION

Naturalness arguments on the spectrum of SUSY theories require the masses of higgsinos to be small, i.e. below the TeV scale. In this context one would also expect a compressed spectrum, where the LSP ( $\tilde{\chi}_1^0$ ), the lightest chargino ( $\tilde{\chi}_1^\pm$ ) and the next-to-lightest neutralino ( $\tilde{\chi}_2^0$ ) are close in mass. Experimental analyses with the largest sensitivity to this kind of scenario consider three main processes, which all lead to signatures with soft leptons and moderate missing transverse momentum in the final state [10]. The first two processes are the associated production of a  $\tilde{\chi}_2^0$  and a positively or negatively charged  $\tilde{\chi}_1^\pm$ , while in the third process a pair of neutralinos ( $\tilde{\chi}_2^0\tilde{\chi}_1^0$ ) is produced. The heavier neutralino  $\tilde{\chi}_2^0$  and the charginos  $\tilde{\chi}_1^\pm$  will decay to the lighter  $\tilde{\chi}_1^0$  through an off-shell  $Z$  or  $W^\pm$  boson, respectively. Since the decay products are expected to be soft because of the compressed spectrum, a jet with large transverse momentum produced through initial state radiation can enhance the discriminating power with respect to SM processes [10].

In the following, we consistently compute the cross sections for the aforementioned processes at NLO+NLL adopting threshold-improved PDFs and the  $K$ -factor method described in Sec. II. The spectra with the specific characteristics of this scenario have been obtained with the public code SPheno [56, 57], following the considerations in Ref. [13]. In particular, light higgsino-like neutralinos and charginos  $\tilde{\chi}_1^0$ ,  $\tilde{\chi}_1^\pm$  and  $\tilde{\chi}_2^0$  of masses similar to the higgsino mass parameter  $\mu$  can be obtained by setting this parameter to  $\mu \leq M_1 = M_2$ , i.e. below the bino and wino mass parameters  $M_1$  and  $M_2$ . We choose  $\mu$  between 100 GeV and 500 GeV in order to stay (not too far) above the experimental exclusion limits, while our choice  $M_{1,2} = 1$  TeV ensures a large higgsino content and mass splittings of the order of 5 GeV (i.e.  $m_{\tilde{\chi}_2^0} - m_{\tilde{\chi}_1^\pm} \approx m_{\tilde{\chi}_1^\pm} - m_{\tilde{\chi}_1^0} \approx 5$  GeV). Our calculations of differential and total cross sections at NLO+NLL are performed using RESUMMINO [48] interfaced with LHAPDF6 [58] for the interpolation of the PDF grids. The SM parameters have been chosen according to their current PDG values [59], and we fix  $\alpha_s(M_Z) = 0.118$  with  $\Lambda_{n_f=5}^{\overline{\text{MS}}} = 0.239$  GeV as appropriate for NNPDF3.0.

We begin with the invariant-mass distribution for the associated production of a second-lightest neutralino and the lightest positive chargino ( $\tilde{\chi}_2^0\tilde{\chi}_1^+$ ). These differential cross sections at LO, NLO and NLO+NLL computed with the global NNPDF3.0 PDF set are shown in the upper panel of Fig. 1. Comparing the LO and NLO curves we observe an increase of about 20% in the low invariant mass region and of about 10% at higher invariant masses. A further enhancement of about 1% and 4% reflects the effect of the resummation in the NLO+NLL curve compared with the NLO result in the low and high invariant-mass regions, respectively. In the lower panel of Fig. 1 we show the  $K$ -factor that has been defined in

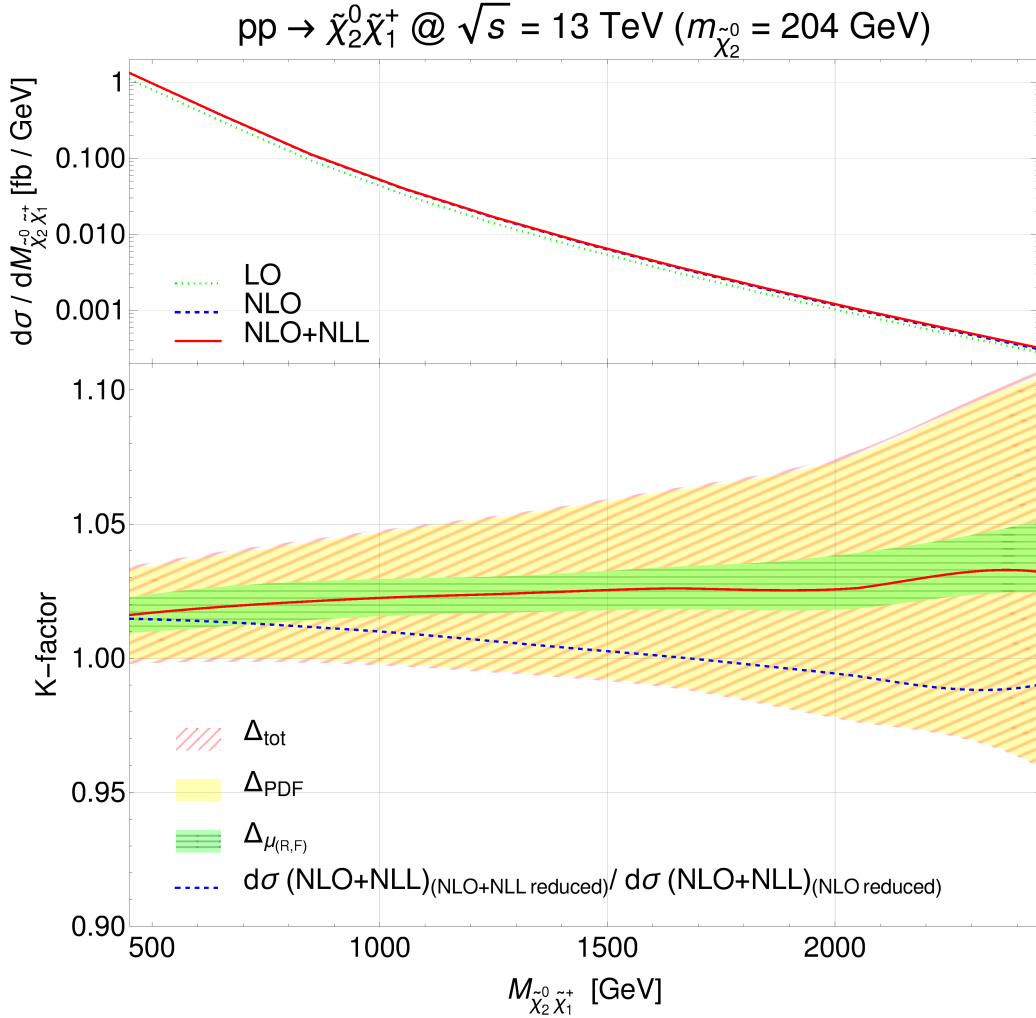


FIG. 1. Invariant-mass distributions (upper panel) and  $K$ -factors (lower panel) according to Eq. (2.1) using the full expression (full red) and only its second, PDF-dependent part (dashed blue line) for  $\tilde{\chi}_2^0 \tilde{\chi}_1^+$  production at the LHC with  $\sqrt{s} = 13$  TeV. The higgsino masses are  $m_{\tilde{\chi}_2^0} = 204$  GeV and  $m_{\tilde{\chi}_1^+} = 199$  GeV. In the upper panel, the results at LO (dotted green), NLO (dashed blue) and NLO+NLL (full red line) have been obtained with global NLO PDFs. In the lower panel, the PDF (yellow band) and scale (horizontally dashed green band) uncertainties have been computed at NLO and NLO+NLL, respectively, with global NLO PDFs, then rescaled appropriately and added in quadrature for the total theoretical uncertainty (diagonally dashed red band).

Eq. (2.1) (full red) as well as the contribution of its second term only (dashed blue line), which highlights the effect of the resummation within the PDF fits. In the low invariant-mass region, the two curves are similar and predict an increase of the cross section from the global fixed-order results of about 1.5%. This can be explained by the observation that far from threshold resummation effects are small both in the PDFs and even more so in the partonic matrix elements. In the high invariant-mass region, the resummation effects in the PDFs reduce the total cross section (dashed blue), partially compensating those of the

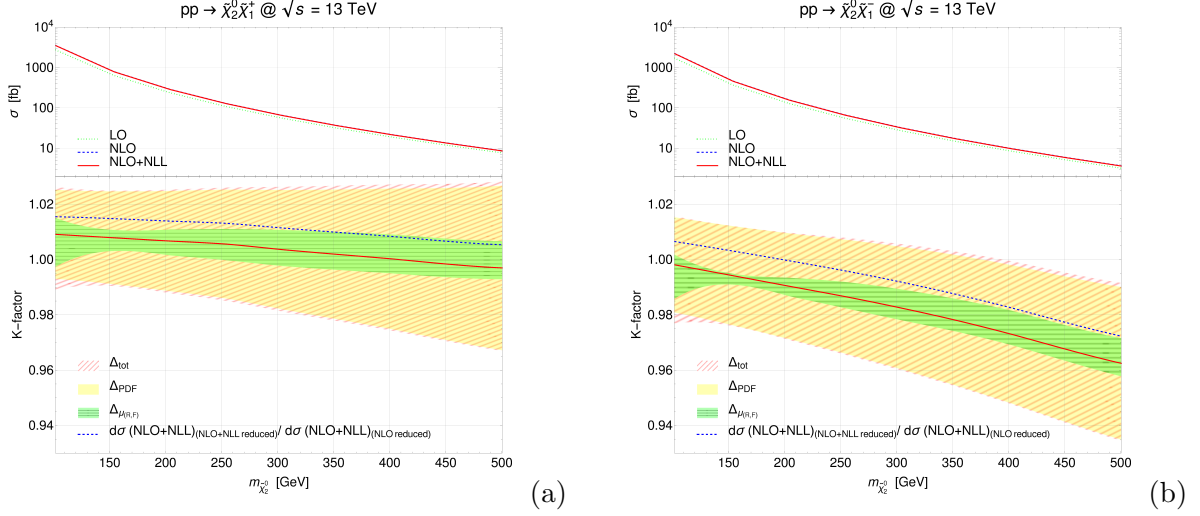


FIG. 2. Same as Fig. 1, but for the total cross sections of the associated production of second-lightest neutralinos with positive (left) and negative (right) charginos as a function of the neutralino mass. The chargino is always about 5 GeV lighter.

partonic matrix elements in the total result (full red curve). The overall effect is an increase of the fixed-order result by about 3%. The error bands represent the PDF (yellow band) and scale uncertainties (horizontally dashed green band). They have been calculated and combined into the total theoretical uncertainty (diagonally dashed red band) following the procedure explained in Sec. II. As one would expect, the PDF error grows at high invariant masses due to the larger uncertainties of the PDFs in the high- $x$  region, whereas the scale error is considerably smaller and stays relatively constant.

Following the same procedure, we show in Fig. 2 total cross sections for the associated production of the second-lightest neutralino and the lightest chargino ( $\tilde{\chi}_2^0 \tilde{\chi}_1^\pm$ ) as function of the mass of the neutralino. The chargino is always about 5 GeV lighter. We present the results for both positive (left) and negative (right) chargino production. As expected for a  $pp$  collider such as the LHC, the first of these processes has a larger cross section. Both cross sections are enhanced by the QCD corrections from LO to NLO by about 30% for light higgsino masses and by about 13% as the particles get heavier. The resummation in the partonic matrix elements leads instead to a reduction of the cross section by about 1% almost independently of the higgsino masses. In the lower panels we plot the  $K$ -factors of the two processes. They show different trends. For positive chargino production (left), the introduction of the new resummed PDF set (dashed blue line) further increases the cross section by about 1.5% at low electroweakino masses and of about 0.5% at higher masses. This effect is partially compensated by the effect of the resummation in the partonic matrix elements, such that in the end we observe a positive correction to the fixed order NLO cross section obtained from the global PDF set of less than 1% for light higgsino masses and a negative correction of less than 0.5% for heavier masses. The results are different in the case of negative chargino production (right). The resummation in the PDFs brings a positive correction to the cross section of about 0.5% only for very light higgsino masses, and it rapidly turns to negative values as the higgsinos get heavier and then reaches a negative correction of about 3%. This correction gets accentuated by the effect of the resummation

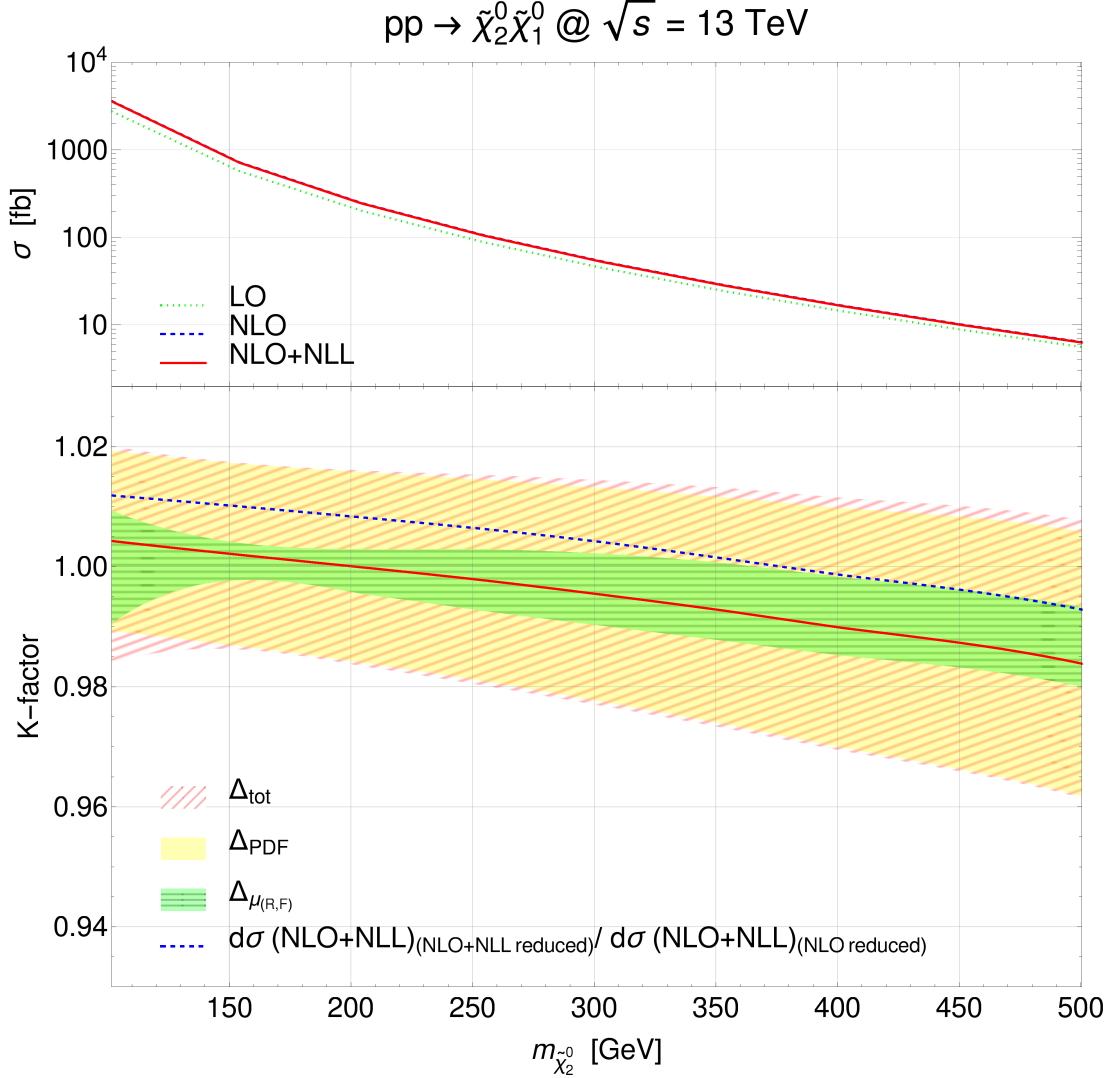


FIG. 3. Same as Fig. 2 for total cross sections of the associated production of second-lightest neutralinos with the lightest neutralino as a function of the mass of the former. The latter is always about 10 GeV lighter.

in the partonic matrix elements, so that for light higgsino masses the  $K$ -factor is close to unity, while for heavier masses it gives a negative correction of about 4%. In both cases, the total theoretical uncertainty is dominated by the PDF error, which grows towards larger higgsino masses, while the scale error stays again relatively constant.

In the higgsino scenario, we also consider the process for the associated production of two neutralinos  $\tilde{\chi}_2^0 \tilde{\chi}_1^0$ . In the upper panel of Fig. 3, we show the cross sections for this process at LO, NLO and NLO+NLL obtained with the global NNPDF3.0 set. The effect of QCD corrections is similar to what we have found in the previous cases. They produce an enhancement of the cross section from LO to NLO of about 30% for light higgsinos and of about 13% for heavier masses. The resummation decreases the cross section by about 1% when going from NLO to NLO+NLL independently on the higgsino mass. In the lower

$m_{\tilde{\chi}_2^0}$ [GeV]	$m_{\tilde{\chi}_1^\pm}$ [GeV]	LO (LO global) [fb]	NLO (NLO global) [fb]	NLO+NLL (id. global) [fb]
101.5	96.2	$2733^{+4.4\%}_{-5.4\%} \pm 6.3\%$	$3545^{+2.1\%}_{-1.7\%} \pm 1.6\%$	$3577^{+0.6\%}_{-1.2\%} \pm 1.6\%$
154.2	148.9	$630^{+1.3\%}_{-2.0\%} \pm 6.2\%$	$784^{+1.8\%}_{-1.5\%} \pm 1.7\%$	$790^{+0.3\%}_{-0.5\%} \pm 1.7\%$
204.5	199.0	$234^{+0.0\%}_{-0.4\%} \pm 6.3\%$	$284^{+1.9\%}_{-1.3\%} \pm 1.8\%$	$286^{+0.4\%}_{-0.5\%} \pm 1.8\%$
254.3	248.5	$107^{+1.4\%}_{-1.7\%} \pm 6.3\%$	$127^{+2.0\%}_{-1.5\%} \pm 1.9\%$	$128^{+0.5\%}_{-0.6\%} \pm 1.9\%$
303.9	297.7	$55.3^{+2.5\%}_{-2.6\%} \pm 6.4\%$	$65.0^{+2.1\%}_{-1.7\%} \pm 2.2\%$	$65.2^{+0.7\%}_{-0.6\%} \pm 2.2\%$
353.4	346.7	$31.2^{+3.5\%}_{-3.4\%} \pm 6.4\%$	$36.2^{+2.1\%}_{-1.9\%} \pm 2.3\%$	$36.2^{+0.8\%}_{-0.6\%} \pm 2.3\%$
402.6	395.3	$18.7^{+4.3\%}_{-4.0\%} \pm 6.5\%$	$21.4^{+2.2\%}_{-2.0\%} \pm 2.5\%$	$21.4^{+0.9\%}_{-0.5\%} \pm 2.5\%$
451.6	443.6	$11.7^{+4.9\%}_{-4.6\%} \pm 6.6\%$	$13.3^{+2.2\%}_{-2.1\%} \pm 2.8\%$	$13.3^{+0.9\%}_{-0.5\%} \pm 2.8\%$
500.4	491.5	$7.61^{+5.6\%}_{-5.1\%} \pm 6.6\%$	$8.59^{+2.3\%}_{-2.3\%} \pm 3.0\%$	$8.57^{+1.0\%}_{-0.4\%} \pm 3.0\%$

TABLE I. Total cross sections for associated  $\tilde{\chi}_2^0\tilde{\chi}_1^\pm$  production at the LHC with  $\sqrt{s} = 13$  TeV at LO, NLO and NLO+NLL with consistent PDF choices. The central NLO+NLL results are obtained with the  $K$ -factor method as well as the PDF (symmetric) uncertainty at NLO (identical in the last two columns), whereas the NLO+NLL (asymmetric) scale uncertainty has been computed directly.

panel, we can see that the effect of the threshold-improved PDFs (blue dashed curve) ranges between  $\pm 1\%$  over the neutralino mass range, while the overall effect of the resummation, both in the PDFs and in the partonic matrix elements (full red curve), leads to a positive correction of the order of 0.5% for light neutralinos and a negative correction of the order of 1.5% for heavier masses. The behaviour of the PDF, scale and total theoretical uncertainties is again similar as before.

We summarise the results of this section by giving explicit values for the integrated cross sections for the three described processes in Tabs. I, II and III. We include the theoretical uncertainties that have been calculated following the procedure described in Sec. II. The symmetric PDF errors on the NLO+NLL cross sections are derived from the application of the  $K$ -factor, thus their relative size will be the same for the fixed order and the resummed results. The asymmetric scale uncertainties instead have been explicitly estimated in each case through the seven-point method. Following this approach, the benefits of the resummation on the uncertainty from scale variation are clearly visible.

#### IV. GAUGINO PAIR PRODUCTION

We now turn to the case where the produced neutralinos and charginos have a large gaugino component. The next-to-lightest neutralino  $\tilde{\chi}_2^0$  and the charginos  $\tilde{\chi}_1^\pm$  will be considered as wino-like and almost degenerate with a mass above 760 GeV to satisfy experimental constraints, while the LSP  $\tilde{\chi}_1^0$  is assumed to be bino-like and light. In this scenario, large production cross sections of  $\tilde{\chi}_2^0\tilde{\chi}_1^\pm$  and short decay chains are expected. Assuming an intermediate and equal mass for left-handed staus and tau sneutrinos, the winos will decay through these states into the LSP, taus and tau neutrinos, leading to interesting collider signatures [7]. This particular spectrum of particle masses can be achieved within the phenomenological MSSM (pMSSM) framework. It is of particular interest, since the coannihilation of light staus with the LSP can generate a dark matter relic density in accordance with the observations.



$m_{\tilde{\chi}_2^0}$ [GeV]	$m_{\tilde{\chi}_1^-}$ [GeV]	LO (LO global) [fb]	NLO (NLO global) [fb]	NLO+NLL (id. global) [fb]
101.5	96.2	$1712^{+4.6\%}_{-5.7\%} \pm 6.6\%$	$2244^{+2.1\%}_{-1.7\%} \pm 1.7\%$	$2240^{+0.4\%}_{-1.2\%} \pm 1.7\%$
154.2	148.9	$363^{+1.5\%}_{-2.2\%} \pm 6.6\%$	$457^{+1.7\%}_{-1.4\%} \pm 1.8\%$	$455^{+0.1\%}_{-0.3\%} \pm 1.8\%$
204.5	199.0	$127^{+0.0\%}_{-0.4\%} \pm 6.7\%$	$155^{+1.9\%}_{-1.3\%} \pm 1.9\%$	$154^{+0.3\%}_{-0.4\%} \pm 1.9\%$
254.3	248.5	$54.8^{+1.4\%}_{-1.7\%} \pm 6.7\%$	$66.0^{+2.0\%}_{-1.5\%} \pm 2.1\%$	$65.1^{+0.5\%}_{-0.4\%} \pm 2.1\%$
303.9	297.7	$27.0^{+2.6\%}_{-2.7\%} \pm 6.8\%$	$32.0^{+2.1\%}_{-1.7\%} \pm 2.3\%$	$31.5^{+0.7\%}_{-0.4\%} \pm 2.3\%$
353.4	346.7	$14.6^{+3.5\%}_{-3.5\%} \pm 6.9\%$	$17.1^{+2.1\%}_{-1.8\%} \pm 2.4\%$	$16.7^{+0.8\%}_{-0.4\%} \pm 2.4\%$
402.6	395.3	$8.38^{+4.3\%}_{-4.2\%} \pm 7.1\%$	$9.72^{+2.2\%}_{-2.0\%} \pm 2.6\%$	$9.45^{+0.9\%}_{-0.4\%} \pm 2.6\%$
451.6	443.6	$5.06^{+5.1\%}_{-4.7\%} \pm 7.3\%$	$5.82^{+2.2\%}_{-2.1\%} \pm 2.7\%$	$5.63^{+0.9\%}_{-0.4\%} \pm 2.7\%$
500.4	491.5	$3.18^{+5.7\%}_{-5.2\%} \pm 7.5\%$	$3.63^{+2.3\%}_{-2.3\%} \pm 2.9\%$	$3.50^{+0.9\%}_{-0.5\%} \pm 2.9\%$

TABLE II. Same as Tab. I, but for associated  $\tilde{\chi}_2^0\tilde{\chi}_1^-$  production.

$m_{\tilde{\chi}_2^0}$ [GeV]	$m_{\tilde{\chi}_1^0}$ [GeV]	LO (LO global) [fb]	NLO (NLO global) [fb]	NLO+NLL (id. global) [fb]
101.5	92.1	$2770^{+5.0\%}_{-6.0\%} \pm 6.4\%$	$3633^{+2.2\%}_{-1.8\%} \pm 1.5\%$	$3649^{+0.5\%}_{-1.4\%} \pm 1.5\%$
154.2	144.4	$574^{+1.6\%}_{-2.4\%} \pm 6.3\%$	$721^{+1.8\%}_{-1.5\%} \pm 1.5\%$	$722^{+0.2\%}_{-0.4\%} \pm 1.5\%$
204.5	194.4	$202^{+0.0\%}_{-0.3\%} \pm 6.3\%$	$247^{+1.9\%}_{-1.3\%} \pm 1.6\%$	$247^{+0.3\%}_{-0.4\%} \pm 1.6\%$
254.3	243.9	$88.6^{+1.3\%}_{-1.6\%} \pm 6.3\%$	$106^{+2.0\%}_{-1.5\%} \pm 1.7\%$	$106^{+0.5\%}_{-0.5\%} \pm 1.7\%$
303.9	293.1	$44.5^{+2.4\%}_{-2.6\%} \pm 6.3\%$	$52.6^{+2.0\%}_{-1.7\%} \pm 1.8\%$	$52.3^{+0.7\%}_{-0.5\%} \pm 1.8\%$
353.4	342.0	$24.4^{+3.4\%}_{-3.4\%} \pm 6.3\%$	$28.5^{+2.1\%}_{-1.9\%} \pm 1.9\%$	$28.3^{+0.8\%}_{-0.5\%} \pm 1.9\%$
402.6	390.6	$14.3^{+4.2\%}_{-4.0\%} \pm 6.3\%$	$16.5^{+2.2\%}_{-2.0\%} \pm 2.0\%$	$16.3^{+0.9\%}_{-0.5\%} \pm 2.0\%$
451.6	438.7	$8.77^{+4.9\%}_{-4.6\%} \pm 6.3\%$	$10.04^{+2.2\%}_{-2.1\%} \pm 2.1\%$	$9.91^{+0.9\%}_{-0.4\%} \pm 2.1\%$
500.4	486.2	$5.60^{+5.6\%}_{-5.1\%} \pm 6.4\%$	$6.36^{+2.3\%}_{-2.3\%} \pm 2.2\%$	$6.26^{+1.0\%}_{-0.4\%} \pm 2.2\%$

TABLE III. Same as Tab. I, but for associated  $\tilde{\chi}_2^0\tilde{\chi}_1^0$  production.

A spectrum with these features is obtained using the public code SPheno [56, 57] by setting a small value for the bino mass parameter  $M_1$ , while the wino mass parameter  $M_2$  is chosen above the ATLAS exclusion limits. The large gaugino content can be achieved by setting a large value for the  $\mu$  parameter ( $\mu \gg M_2$ ). With this configuration, only a very small splitting between the masses of the neutralino  $\tilde{\chi}_2^0$  and the charginos  $\tilde{\chi}_1^\pm$  is generated.

We now study the effect of the inclusion of threshold-resummed PDFs in a consistent calculation of the cross sections at NLO+NLL. We first consider a specific configuration of the masses and study the invariant-mass distribution for  $\tilde{\chi}_2^0\tilde{\chi}_1^+$  associated production. In Fig. 4, the upper panel shows the invariant mass distributions calculated at LO, NLO and NLO+NLL with the global NNPDF3.0 PDF set. Here, QCD corrections have a large impact on the cross section, which increases from LO to NLO by about 80% and 30% at low and high invariant masses, respectively. The resummation further increases the cross section by about 6% in the low invariant-mass region and by about 10% for higher invariant masses. Resummation effects in the PDFs only (dashed blue line) are small as they remain below 2.5% over the whole invariant-mass region considered here. In the same interval, resummation in the partonic matrix elements gives a large contribution and produces an

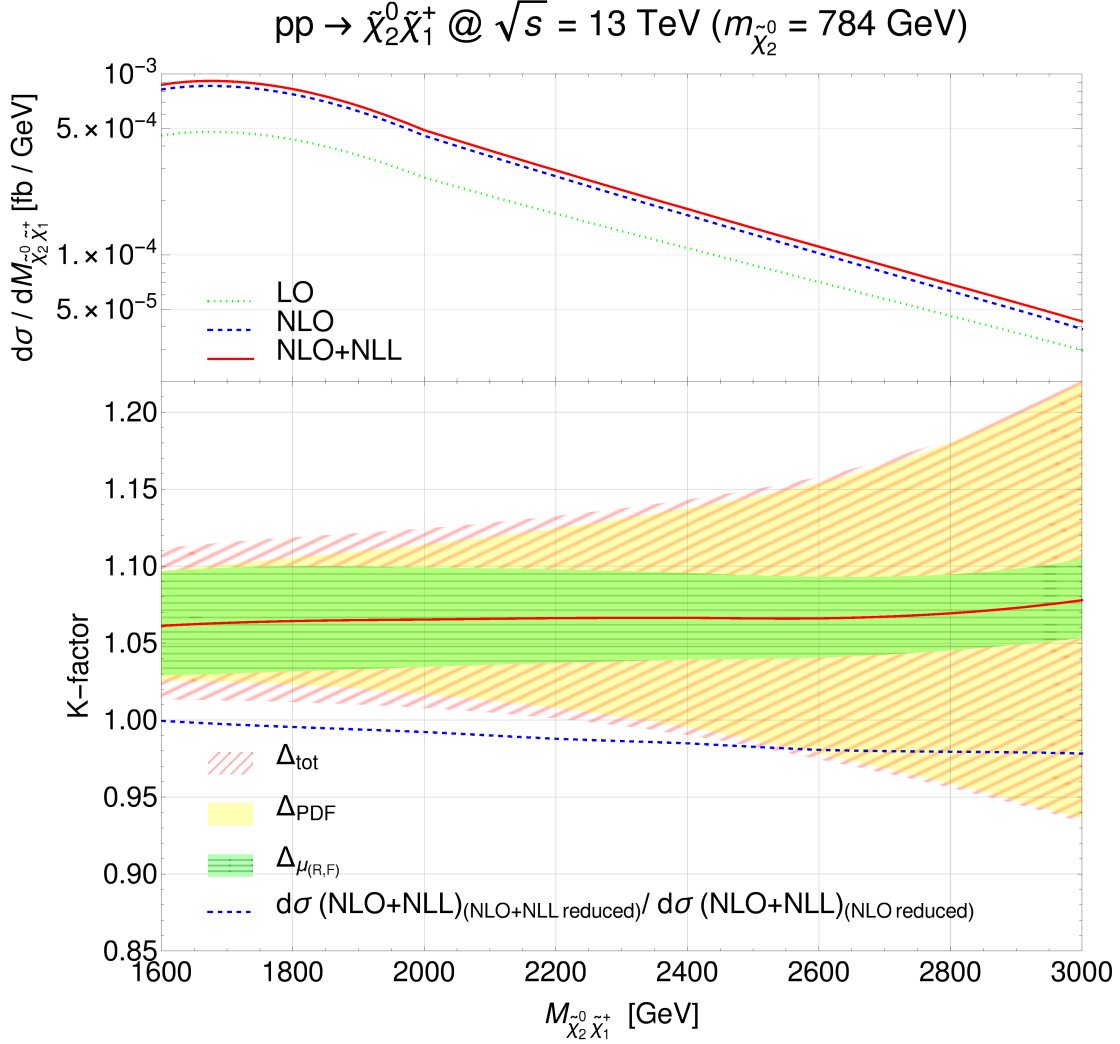


FIG. 4. Invariant-mass distributions (upper panel) and  $K$ -factors (lower panel) according to Eq. (2.1) using the full expression (full red) and only its second, PDF-dependent part (dashed blue line) for  $\tilde{\chi}_2^0 \tilde{\chi}_1^+$  associated production at the LHC with  $\sqrt{s} = 13$  TeV. The wino masses are  $m_{\tilde{\chi}_2^0} \simeq m_{\tilde{\chi}_1^+} = 784$  GeV. In the upper panel, the results at LO (dotted green), NLO (dashed blue) and NLO+NLL (full red line) have been obtained with global NLO PDFs. In the lower panel, the PDF (yellow band) and scale (horizontally dashed green band) uncertainties have been computed at NLO and NLO+NLL, respectively, with global NLO PDFs, then rescaled appropriately and added in quadrature for the total theoretical uncertainty (diagonally dashed red band).

enhancement of the cross section between 6% and 8%. The reason is that the winos in this section are considerably heavier than the higgsinos in the preceding section, so that we are closer to threshold and resummation effects are more important.

We repeat the analysis to study the effects of resummed PDFs on the integrated cross section. The results are shown in Fig. 5. In the upper plot we can observe the effects of the QCD corrections, which are large for light winos and enhance the cross section from LO to NLO by about 65%. The enhancement then rapidly decreases for heavier masses. The

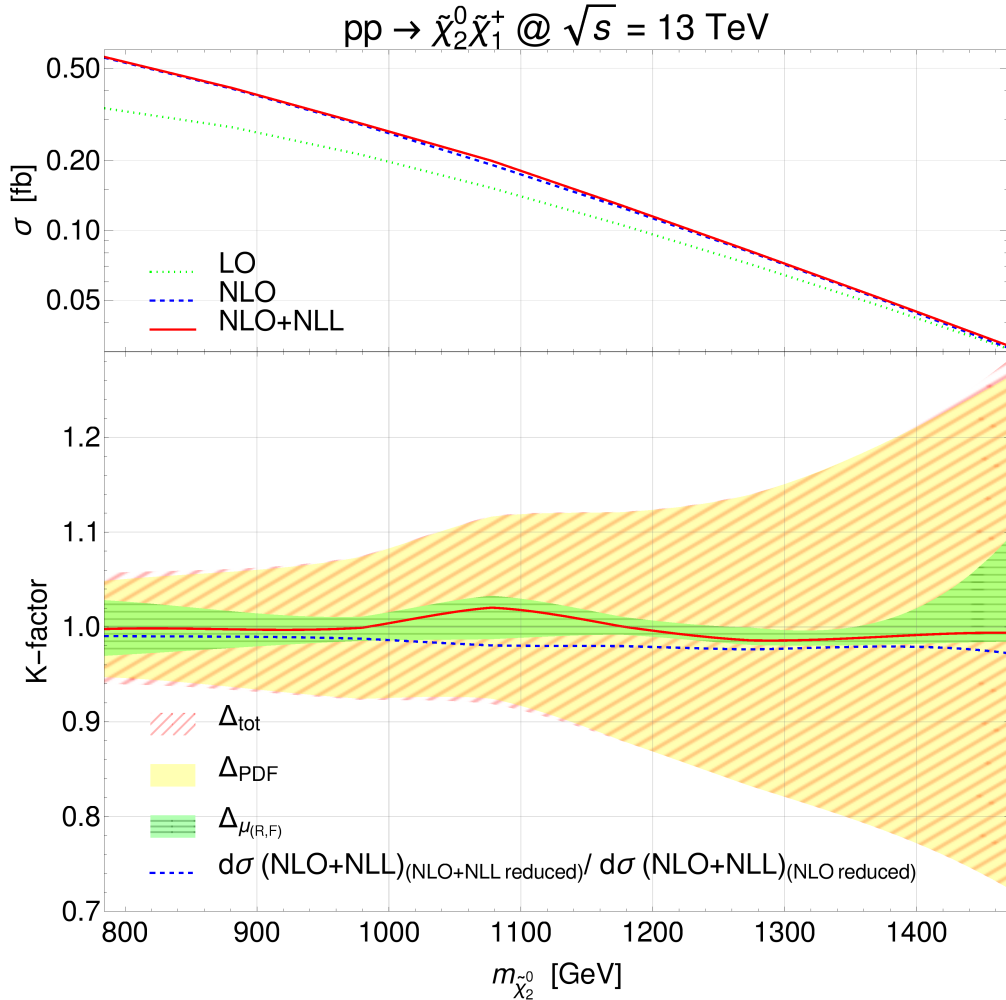


FIG. 5. Same as Fig. 2, but for the total cross sections of the associated production of second-lightest neutralinos with positive charginos as a function of their mass.

effect of the resummation further increases the cross section from NLO to NLO+NLL by about 2% to 4% in the wino mass range considered here. The effect of the resummation in the PDFs (dashed blue line) is small in this scenario, and the combined effect with the resummation in the partonic matrix elements is dominated by the latter and again it brings a positive contribution to the cross section between 2% and 4% in the whole considered wino mass range.

We conclude this section by giving explicit results for the cross sections at LO, NLO and NLO+NLL in Tab. IV. They have been consistently calculated through the  $K$ -factor method in this scenario of neutralinos and gauginos with large gaugino content.

$m_{\tilde{\chi}_2^0}$ [GeV]	LO (LO global) [fb]	NLO (NLO global) [fb]	NLO+NLL (id. global) [fb]
784.2	$0.336^{+8.6\%}_{-7.5\%} \pm 7.6\%$	$0.556^{+8.6\%}_{-7.3\%} \pm 5.1\%$	$0.554^{+3.1\%}_{-2.8\%} \pm 5.1\%$
881.8	$0.278^{+9.2\%}_{-8.0\%} \pm 8.0\%$	$0.407^{+7.6\%}_{-6.7\%} \pm 6.1\%$	$0.406^{+1.9\%}_{-2.0\%} \pm 6.1\%$
979.8	$0.211^{+9.9\%}_{-8.5\%} \pm 8.7\%$	$0.284^{+7.0\%}_{-6.3\%} \pm 7.5\%$	$0.284^{+1.2\%}_{-1.4\%} \pm 7.5\%$
1078	$0.152^{+10.6\%}_{-9.1\%} \pm 9.6\%$	$0.192^{+6.6\%}_{-6.1\%} \pm 9.4\%$	$0.196^{+1.2\%}_{-3.3\%} \pm 9.4\%$
1176	$0.106^{+11.3\%}_{-9.6\%} \pm 10.8\%$	$0.126^{+6.4\%}_{-6.1\%} \pm 12.0\%$	$0.126^{+1.0\%}_{-0.9\%} \pm 12.0\%$
1274	$0.071^{+12.0\%}_{-10.1\%} \pm 12.4\%$	$0.080^{+6.3\%}_{-6.1\%} \pm 15.6\%$	$0.079^{+1.4\%}_{-0.5\%} \pm 15.6\%$
1372	$0.047^{+12.6\%}_{-10.6\%} \pm 14.5\%$	$0.050^{+6.3\%}_{-6.1\%} \pm 20.5\%$	$0.050^{+1.7\%}_{-0.8\%} \pm 20.5\%$
1470	$0.031^{+13.2\%}_{-11.0\%} \pm 17.2\%$	$0.031^{+6.2\%}_{-6.2\%} \pm 27.2\%$	$0.031^{+10.1\%}_{-1.0\%} \pm 27.2\%$

TABLE IV. Same as Tab. I, but for winos instead of higgsinos.

## V. CONCLUSION

In this paper, we have studied the effects of the introduction of threshold-resummation improved PDF sets in consistent NLO+NLL calculations for the associated production of neutralinos and charginos at Run II of the LHC. In particular, we computed LO, NLO and NLO+NLL cross sections for various processes relevant for current and future experimental searches. The SUSY particles were considered in two different mass ranges and in scenarios where they featured either a large higgsino or a large gaugino content.

The impact of the resummation within the PDFs has been parametrised through a factorisation method employed previously for squarks, gluinos and sleptons. Using ratios of resummed and fixed-order cross sections in a specific  $K$ -factor, it is easily possible to rescale the fixed-order NLO results to consistent NLO+NLL calculations, which include the effects of the resummation in the partonic matrix elements as well as in the PDF fits. As expected, the use of threshold-resummation improved PDFs partially compensates the enhancement of the cross sections due to the resummation in the partonic matrix elements.

Scale uncertainties and PDF error bands were given along with the central values for the  $K$ -factors. The latter were extracted from the global NNPDF3.0 set in order to minimise the impact of the reduction of the data set in the fit of the threshold-resummation improved PDFs. Through this method, also the troublesome refitting in Mellin space of the NNPDF replicas of the PDF sets from reduced data sets was bypassed. The effects of the variation of factorisation and renormalisation scales were determined explicitly with the corresponding cross sections in order to preserve the benefits of the resummation in terms of the reduction of scale uncertainties.

To conclude, the presented results allow to further improve the reliability of the theoretical calculations for the interpretation of the experimental data during the ongoing LHC Run-II programme.

## ACKNOWLEDGMENTS

This work has been supported by the BMBF under contract 05H15PMCCA and the DFG through the Research Training Network 2149 ‘‘Strong and weak interactions - from hadrons

to dark matter”.

- 
- [1] H. P. Nilles, Phys. Rept. **110**, 1 (1984).
  - [2] H. E. Haber and G. L. Kane, Phys. Rept. **117**, 75 (1985).
  - [3] M. Klasen, M. Pohl, and G. Sigl, Prog. Part. Nucl. Phys. **85**, 1 (2015), arXiv:1507.03800 [hep-ph].
  - [4] B. Fuks, B. Herrmann, and M. Klasen, Nucl. Phys. **B810**, 266 (2009), arXiv:0808.1104 [hep-ph].
  - [5] B. Herrmann, M. Klasen, and K. Kovarik, Phys. Rev. **D79**, 061701 (2009), arXiv:0901.0481 [hep-ph].
  - [6] B. Herrmann, M. Klasen, and K. Kovarik, Phys. Rev. **D80**, 085025 (2009), arXiv:0907.0030 [hep-ph].
  - [7] M. Aaboud *et al.* (ATLAS), Eur. Phys. J. **C78**, 154 (2018), arXiv:1708.07875 [hep-ex].
  - [8] A. M. Sirunyan *et al.* (CMS), Phys. Lett. **B780**, 118 (2018), arXiv:1711.08008 [hep-ex].
  - [9] M. Aaboud *et al.* (ATLAS), (2018), arXiv:1804.03602 [hep-ex].
  - [10] A. M. Sirunyan *et al.* (CMS), (2018), arXiv:1801.01846 [hep-ex].
  - [11] J. Alwall, P. Schuster, and N. Toro, Phys. Rev. **D79**, 075020 (2009), arXiv:0810.3921 [hep-ph].
  - [12] L. Calibbi, J. M. Lindert, T. Ota, and Y. Takanishi, JHEP **11**, 106 (2014), arXiv:1410.5730 [hep-ph].
  - [13] B. Fuks, M. Klasen, S. Schmiemann, and M. Sunder, (2017), arXiv:1710.09941 [hep-ph].
  - [14] W. Beenakker, R. Hopker, M. Spira, and P. M. Zerwas, Nucl. Phys. **B492**, 51 (1997), arXiv:hep-ph/9610490 [hep-ph].
  - [15] W. Beenakker, M. Kramer, T. Plehn, M. Spira, and P. M. Zerwas, Nucl. Phys. **B515**, 3 (1998), arXiv:hep-ph/9710451 [hep-ph].
  - [16] W. Beenakker, M. Klasen, M. Kramer, T. Plehn, M. Spira, and P. M. Zerwas, Phys. Rev. Lett. **83**, 3780 (1999), [Erratum: Phys. Rev. Lett. 100, 029901 (2008)], arXiv:hep-ph/9906298 [hep-ph].
  - [17] E. L. Berger, M. Klasen, and T. M. P. Tait, Phys. Lett. **B459**, 165 (1999), arXiv:hep-ph/9902350 [hep-ph].
  - [18] E. L. Berger, M. Klasen, and T. M. P. Tait, Phys. Rev. **D62**, 095014 (2000), [Erratum: Phys. Rev. D67, 099901 (2003)], arXiv:hep-ph/0212306 [hep-ph].
  - [19] M. Spira, in *Supersymmetry and unification of fundamental interactions. Proceedings, 10th International Conference, SUSY'02, Hamburg, Germany, June 17-23, 2002* (2002) pp. 217–226, arXiv:hep-ph/0211145 [hep-ph].
  - [20] L. G. Jin, C. S. Li, and J. J. Liu, Phys. Lett. **B561**, 135 (2003), arXiv:hep-ph/0307390 [hep-ph].
  - [21] T. Binoth, D. Goncalves Netto, D. Lopez-Val, K. Mawatari, T. Plehn, and I. Wigmore, Phys. Rev. **D84**, 075005 (2011), arXiv:1108.1250 [hep-ph].
  - [22] A. I. Ahmadov and M. Demirci, Phys. Rev. **D88**, 015017 (2013), arXiv:1307.3777 [hep-ph].
  - [23] M. Demirci and A. I. Ahmadov, Phys. Rev. **D89**, 075015 (2014), arXiv:1404.0550 [hep-ph].
  - [24] C. S. Li, Z. Li, R. J. Oakes, and L. L. Yang, Phys. Rev. **D77**, 034010 (2008), arXiv:0707.3952 [hep-ph].
  - [25] J. Debove, B. Fuks, and M. Klasen, Phys. Lett. **B688**, 208 (2010), arXiv:0907.1105 [hep-ph].
  - [26] J. Debove, B. Fuks, and M. Klasen, Nucl. Phys. **B842**, 51 (2011), arXiv:1005.2909 [hep-ph].

- [27] J. Debove, B. Fuks, and M. Klasen, Nucl. Phys. **B849**, 64 (2011), arXiv:1102.4422 [hep-ph].
- [28] B. Fuks, M. Klasen, D. R. Lamprea, and M. Rothering, JHEP **10**, 081 (2012), arXiv:1207.2159 [hep-ph].
- [29] B. Fuks, M. Klasen, and M. Rothering, JHEP **07**, 053 (2016), arXiv:1604.01023 [hep-ph].
- [30] L. L. Yang, C. S. Li, J. J. Liu, and Q. Li, Phys. Rev. **D72**, 074026 (2005), arXiv:hep-ph/0507331 [hep-ph].
- [31] A. Broggio, M. Neubert, and L. Vernazza, JHEP **05**, 151 (2012), arXiv:1111.6624 [hep-ph].
- [32] G. Bozzi, B. Fuks, and M. Klasen, Phys. Rev. **D74**, 015001 (2006), arXiv:hep-ph/0603074 [hep-ph].
- [33] G. Bozzi, B. Fuks, and M. Klasen, Nucl. Phys. **B777**, 157 (2007), arXiv:hep-ph/0701202 [hep-ph].
- [34] G. Bozzi, B. Fuks, and M. Klasen, Nucl. Phys. **B794**, 46 (2008), arXiv:0709.3057 [hep-ph].
- [35] B. Fuks, M. Klasen, D. R. Lamprea, and M. Rothering, JHEP **01**, 168 (2014), arXiv:1310.2621.
- [36] M. Bonvini, S. Marzani, J. Rojo, L. Rottoli, M. Ubiali, R. D. Ball, V. Bertone, S. Carrazza, and N. P. Hartland, JHEP **09**, 191 (2015), arXiv:1507.01006 [hep-ph].
- [37] J. Fiaschi and M. Klasen, JHEP **03**, 094 (2018), arXiv:1801.10357 [hep-ph].
- [38] W. Beenakker, C. Borschensky, M. Kramer, A. Kulesza, E. Laenen, V. Theeuwes, and S. Thewes, JHEP **12**, 023 (2014), arXiv:1404.3134 [hep-ph].
- [39] C. Borschensky, M. Kramer, A. Kulesza, M. Mangano, S. Padhi, T. Plehn, and X. Portell, Eur. Phys. J. **C74**, 3174 (2014), arXiv:1407.5066 [hep-ph].
- [40] M. Beneke, J. Piclum, C. Schwinn, and C. Wever, JHEP **10**, 054 (2016), arXiv:1607.07574 [hep-ph].
- [41] W. Beenakker, C. Borschensky, M. Kramer, A. Kulesza, and E. Laenen, JHEP **12**, 133 (2016), arXiv:1607.07741 [hep-ph].
- [42] A. Broggio, A. Ferroglia, M. Neubert, L. Vernazza, and L. L. Yang, JHEP **03**, 066 (2014), arXiv:1312.4540 [hep-ph].
- [43] W. Beenakker, C. Borschensky, R. Heger, M. Kramer, A. Kulesza, and E. Laenen, JHEP **05**, 153 (2016), arXiv:1601.02954 [hep-ph].
- [44] B. Fuks, M. Klasen, F. Ledroit, Q. Li, and J. Morel, Nucl. Phys. **B797**, 322 (2008), arXiv:0711.0749 [hep-ph].
- [45] T. Jezo, M. Klasen, D. R. Lamprea, F. Lyonnet, and I. Schienbein, JHEP **12**, 092 (2014), arXiv:1410.4692 [hep-ph].
- [46] M. Mitra, R. Ruiz, D. J. Scott, and M. Spannowsky, Phys. Rev. **D94**, 095016 (2016), arXiv:1607.03504 [hep-ph].
- [47] M. Klasen, F. Lyonnet, and F. S. Queiroz, Eur. Phys. J. **C77**, 348 (2017), arXiv:1607.06468 [hep-ph].
- [48] B. Fuks, M. Klasen, D. R. Lamprea, and M. Rothering, Eur. Phys. J. **C73**, 2480 (2013), arXiv:1304.0790 [hep-ph].
- [49] R. Gavin, C. Hangst, M. Krmer, M. Mhleitner, M. Pellen, E. Popena, and M. Spira, JHEP **10**, 187 (2013), arXiv:1305.4061 [hep-ph].
- [50] R. Gavin, C. Hangst, M. Krmer, M. Mhleitner, M. Pellen, E. Popena, and M. Spira, Eur. Phys. J. **C75**, 29 (2015), arXiv:1407.7971 [hep-ph].
- [51] B. Jger, A. von Manteuffel, and S. Thier, JHEP **02**, 041 (2015), arXiv:1410.3802 [hep-ph].
- [52] J. Baglio, B. Jger, and M. Kesenheimer, JHEP **07**, 083 (2016), arXiv:1605.06509 [hep-ph].
- [53] J. Baglio, B. Jger, and M. Kesenheimer, JHEP **07**, 055 (2018), arXiv:1711.00730 [hep-ph].

- [54] W. Beenakker, C. Borschensky, M. Kramer, A. Kulesza, E. Laenen, S. Marzani, and J. Rojo, *Eur. Phys. J.* **C76**, 53 (2016), arXiv:1510.00375 [hep-ph].
- [55] R. D. Ball *et al.* (NNPDF), *JHEP* **04**, 040 (2015), arXiv:1410.8849 [hep-ph].
- [56] W. Porod, *Comput. Phys. Commun.* **153**, 275 (2003), arXiv:hep-ph/0301101 [hep-ph].
- [57] W. Porod and F. Staub, *Comput. Phys. Commun.* **183**, 2458 (2012), arXiv:1104.1573 [hep-ph].
- [58] A. Buckley, J. Ferrando, S. Lloyd, K. Nordstrom, B. Page, M. Rufenacht, M. Schonherr, and G. Watt, *Eur. Phys. J.* **C75**, 132 (2015), arXiv:1412.7420 [hep-ph].
- [59] C. Patrignani *et al.* (Particle Data Group), *Chin. Phys.* **C40**, 100001 (2016).